IEEE Photonics Journal
An IEEE Photonics Society Publication

Open Access

Flexible Optical Cross-Connect Structures Supporting WDM Multicast With Multiple Pumps for Multiple Channels

Volume 6, Number 6, December 2014

Danshi Wang
Min Zhang
Ze Li
Yue Cui

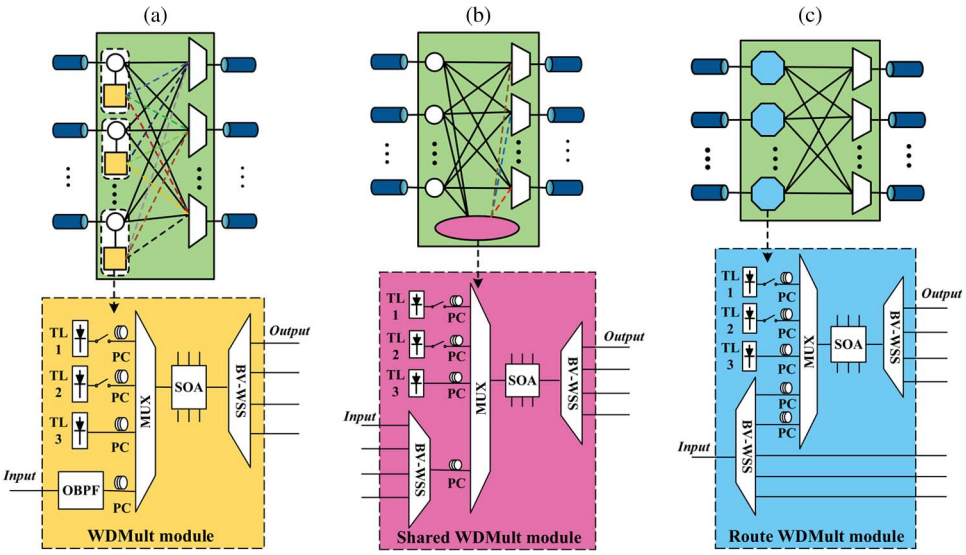

DOI: 10.1109/JPHOT.2014.2374614
1943-0655

IEEE photonics SOCIETY

IEEE

Flexible Optical Cross-Connect Structures Supporting WDM Multicast With Multiple Pumps for Multiple Channels

Danshi Wang, Min Zhang, Ze Li, and Yue Cui

State Key Laboratory of Information Photonics and Optical Communications, Beijing University of Posts and Telecommunications, Beijing 100876, China

DOI: 10.1109/JPHOT.2014.2374614

Manuscript received October 11, 2014; revised November 14, 2014; accepted November 17, 2014. Date of publication November 25, 2014; date of current version December 12, 2014. This work was supported by the NSFC under Project 61372119, by the 863 Program under Grant 2012AA011302, by the Doctoral Scientific Fund Project of the Ministry of Education of China under Grant 20120005110010, and by the BUPT Excellent Ph.D. Students Foundation. Corresponding authors: D. Wang and M. Zhang (e-mail: danshi_wang@bupt.edu.cn; mzhang@bupt.edu.cn).

Abstract: We not only propose three flexible optical cross-connect (OXC) structures, with the ability of wavelength-division multiplexing (WDM) multicast, but also experimentally demonstrate two WDM multicast schemes based on four-wave mixing in a semiconductor optical amplifier (SOA). One-to-ten WDM multicast of 25-Gb/s QPSK signals is achieved with three pumps, and the power penalties for all signals are less than 1.7 dB. For the first time, dual-channel WDM multicasts are simultaneously realized with only two pumps. One-to-six multicast for one input with the largest power penalty of 1.28 dB is obtained, whereas one-to-three multicast for the other input with the power penalty of 1.27 dB is also realized. The demonstrated schemes can be applied to the proposed OXC structures, according to the different requirements. The effect of bias current on conversion efficiency and optical signal-to-noise ratio is also discussed, and the optimal value is given.

Index Terms: All-optical signal processing, WDM multicast, four-wave mixing, semiconductor optical amplifier.

1. Introduction

The exponential growth of high-speed Internet traffic is a constant challenge in optical transport networks. Recently, all-optical wavelength division multiplexing (WDM) multicast, which can efficiently deliver a stream of information from one input wavelength to a number of different output wavelengths, has been regarded as an essential and important function in next-generation all-optical networks, especially for several emerging services such as high definition IP-TV, big data sharing, teaching via the web, data center migration, etc. [1], [2]. Currently, multicast is supported only in the IP layer with larger power consumption and higher cost [3]. The capability of multicast directly in the optical domain at the routing nodes is a target for fast service provisioning, large-grain data flow, and high networks resource efficiency [4]. At first, optical multicast at the fixed wavelength could be easily obtained through a passive power splitter [5]. However, due to the greater multicast bandwidth for big data sharing and data center migration, the natural evolution is toward optical WDM multicast to avoid the wavelength conflict and spectrum resource overlap [6].

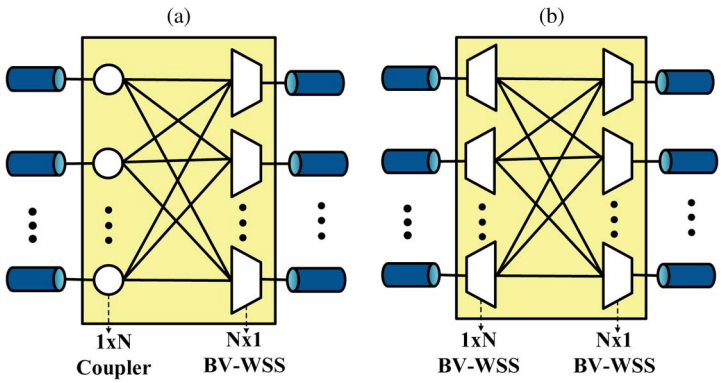

Fig. 1. Two typical OXC structures. (a) Broadcast and select. (b) Route and select.

Recently, several schemes of WDM multicast have been demonstrated by using various nonlinear effects in different devices. For example, signal regeneration with WDM multicast was performed using cross-absorption modulation (XAM) in an electroabsorption modulator (EAM) [7]; Based on self-phase modulation (SPM) in dispersion flattened highly nonlinear photonic crystal fiber (DF-HNL-PCF), one-to-eight WDM multicast was achieved in [8]; By exploiting cross-gain modulation (XGM) in a quantum dot semiconductor optical amplifier (QD-SOA), WDM multicast was demonstrated in [9]. In addition to the aforementioned nonlinear effects, four-wave mixing (FWM) is considered as a promising approach to WDM multicast owing to its transparency to the bit rate and modulation format. FWM-based WDM multicasts were demonstrated in silicon nanowire [10], highly nonlinear fiber (HNLF) [11], [12], photonic crystal fiber (PCF) [13], silicon waveguide [14], and SOA [15]. The 16 QAM and 64 QAM wavelength conversions through FWM have been demonstrated in [16] and [17]. However, due to more complicated interaction process and wider conversion range for more interacted wavelengths, the modulation formats in WDM multicast based on the above mentioned third order nonlinear effects are still limited to OOK or DPSK. Recently, we have achieved one-to-six WDM multicast for QPSK signals through FWM in a SOA [18], [19]. In addition, the second order nonlinear effects, e.g., sum frequency generation (SFG) and difference frequency generation (DFG) occurring in periodically poled lithium niobate waveguide (PPLN), have also been applied in the 16 QAM WDM multicast for the first time [20]. However, according to the reported research work, the highest order modulation format in WDM multicast is 16 QAM by using three pumps to produce only two copies. Furthermore, to the best of our knowledge, all of the proposed schemes of WDM multicast reproduce only one signal to the multiple wavelengths. However, in some situations, there might be more than one signal to be multicast simultaneously. The simultaneous multicast of multiple signals at different wavelengths, which is important for WDM system, has never been reported.

Meanwhile, to cope with the future traffic explosion driven by WDM multicast technology, the development of flexible optical cross-connect (OXC) will be indispensable. Present OXCs mainly utilize the bandwidth variable wavelength selective switch (BV-WSS) for flexible optical networks. Two typical BV-WSS based OXC structures are shown in Fig. 1: (a) “broadcast and select” structure and (b) “route and select” [21]. However, neither of them could perform WDM multicast function. Past WDM multicast researches mainly focused on the physical layer, including nonlinear devices, signal bit rates, modulation formats, and the fold number of multicast [22]. With the development of WDM multicast technology, OXC structures with the ability of WDM multicast need to be addressed.

In this paper, we not only propose three flexible OXC structures supporting WDM multicast according to different situations, but also further extend the WDM multicast experiment through FWM in an SOA based on our previous works. Firstly, one-to-ten WDM multicast of 25 Gbps QPSK signal by applying three pumps is achieved. The largest power penalty is 1.7 dB. Moreover, for the first time, we experimentally demonstrate the simultaneous WDM multicast of two

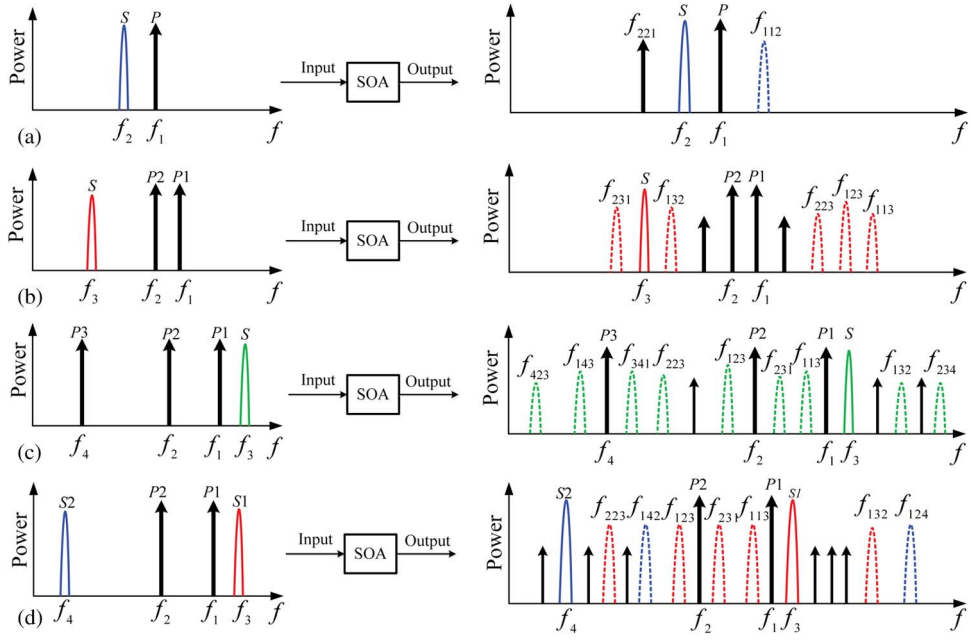

Fig. 2. Operation principle. (a) Wavelength conversion. (b) One-to-six WDM multicast. (c) One-to-ten WDM multicast. (d) Dual-channel WDM multicast.

signals at different wavelengths (dual-channel) in a SOA with only two pumps. One-to-six and one-to-three multicast of 25 Gbps QPSK signals are achieved for the two original signals, respectively. The power penalties for all multicast signals are less than 1.28 dB. The effect of bias current on the performance of multicast signals is also analyzed.

2. Operation Principle

The FWM processes in SOA with different numbers of pumps are schematically illustrated in Fig. 2. Both degenerate FWM (D-FWM) and non-degenerate FWM (ND-FWM) may happen in the SOA. All of the generated components should satisfy the following frequency and phase relationship:

$$f_{abc} = f_a + f_b - f_c \tag{1}$$

$$\varphi_{abc} = \varphi_a + \varphi_b - \varphi_c \tag{2}$$

where f_{abc} and φ_{abc} are the frequency and phase of the generated components ($a \neq c$, $b \neq c$, and a, b, c are selected from the input signals and pumps).

In our schemes, the modulation format of the input signals is QPSK. The single pumped FWM allows the phase mapping from the original signal (S) at f_2 to a converted idler at the different frequency f_{112}, as show in Fig. 2(a) and it is actually the wavelength conversion. Furthermore, the dual-pumped FWM can make the WDM multicast realized, as shown in Fig. 2(b). The frequencies of the two pumps ($P1$ and $P2$) and the original signal (S) are designated as f_1, f_2 and f_3, respectively. After the FWM process, five new idlers preserving the phase information of the original signal will be generated. As above analysis, in order to preserve the phase information of the original QPSK signal, it requires that only one wave carries the original QPSK signal (f_3) among the three waves (f_1, f_2, f_3) participating in FWM process. The three ND-FWM converted idlers $(f_{123}, f_{132}, f_{231})$ and two D-FWM idlers (f_{113}, f_{223}) satisfy the phase-preserving requirement and thus can copy all the information of the original QPSK signal. Therefore one-to-six optical WDM multicast is achieved. According to the similar principle, this time we use three pumps to achieve one-to-ten WDM multicast, as shown in Fig. 2(c). With more pumps, the data carried in

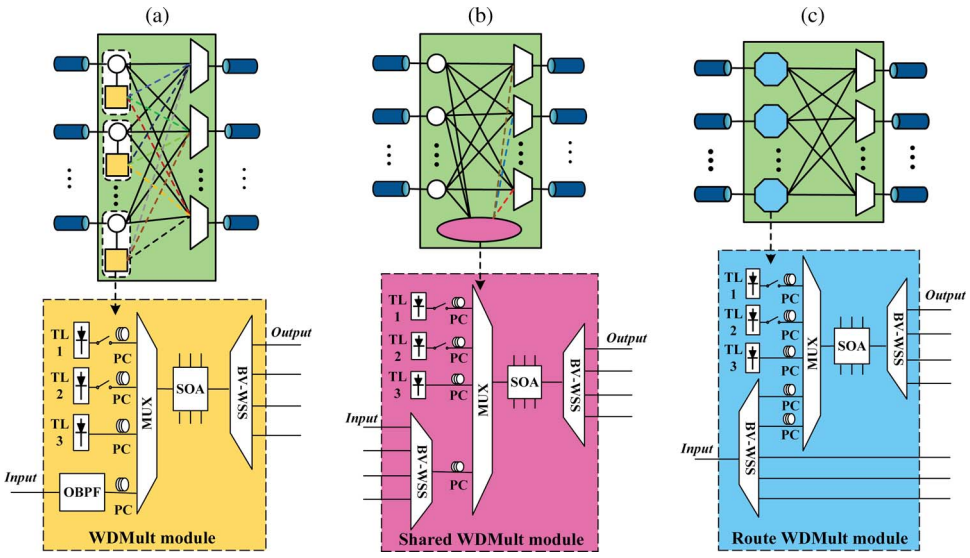

Fig. 3. Three proposed OXC structures. (a) Broadcast and select and WDM multicast. (b) Broadcast and select and partial WDM multicast. (c) Route and select and WDM multicast.

the input signal can be further delivered to more generated FWM components. In order to effectively avoid the crosstalk induced by high-order FWM and beating among the pumps, three pumps need to be placed at the reasonable frequencies and assigned with the appropriate intervals. After the FWM, phase information is preserved and transferred to components at f_{423}, f_{143}, f_{341}, f_{223}, f_{123}, f_{231}, f_{113}, f_{132}, and f_{234}, as shown in Fig. 2(c). Next, the proposed dual-channel WDM multicast based on two-pump FWM in SOA is shown in Fig. 2(d). At the SOA input, there are four FWM participators including two pumps $(P1, P2)$ at frequencies f_1, f_2, and two signals $(S1, S2)$ at f_3, f_4. In order to avoid crosstalk, two pumps and two signals are placed with unequal intervals, i.e., $\Delta f_{42} \neq \Delta f_{21} \neq \Delta f_{13}$. Even so, it is possible to ensure the converted components to be compliant with ITU-T by properly adjusting the frequencies of pumps and signals. Based on FWM, the phase information of $S1$ replicated to the new components at f_{223}, f_{123}, f_{231},f_{113}, and f_{132}; the phase information of $S2$ is transferred to f_{142}, f_{124}, as shown in Fig. 2(d). Therefore, the one-to-six and one-to-three multicast of dual-channel QPSK signals are simultaneously achieved.

3. Structures of OXC With WDM Multicast Module

All of the above-mentioned WDM multicast schemes are based on the all-optical signal processing technique. However, most of the reported all-optical signal processing schemes mainly focused on the physical experiment, without considering the application scenario. We think it is important to implement our WDM multicast schemes in the appropriate optical network scenario to demonstrate its practicality. Therefore, in order to satisfy the requirement of all-optical WDM multicast, we design three OXC structures equipped with WDM multicast module. The first proposed OXC structure is shown in Fig. 3(a): "broadcast and select and WDM multicast," which is modified from the OXC in Fig. 1(a). Each input port is equipped with a WDM multicast module (WDMult module) connected with the corresponding coupler. The WDMult module is described in the orange block diagram consisting of three tunable lasers (TL1 and TL2 and TL3), an optical bandpass filter (OBPF), four polarization controllers (PC), a multiplexer (MUX), a SOA, and a BV-WSS. Compared with other devices, the commercial available SOA is more suitable for the OXC structure for its evident advantages: low cost, integration potential, low input optical power, and high conversion efficiency. Focusing on one input port, an incoming signal can be split and directly broadcasted to all the output ports (solid line). If WDM multicast is needed, the signal will be sent into the WDMult module and coupled with two or three pumps from TL1, TL2, and TL3. After FWM in SOA, at least six multicast signals can be generated at different

wavelengths, then multicast signals are demultiplexed by a BV-WSS and routed to the destination ports (colored dotted line). The programmable BV-WSSs in the structure are properly configured to filter or block the signal. The first OXC can achieve unicast, broadcast, and single-channel WDM multicast in the flexible optical networks.

However, in most cases the WDM multicast is not always necessary for every input signal. When the spectrum resource is abundant and wavelength doesn't conflict, multicast at the same wavelength by a splitter is more practicable [5]. In this situation, only a few signals need WDM multicast. In the OXC of Fig. 3(a), the redundant WDMult modules in each port increase the cost. Therefore, we propose a cost-effective OXC structure shown in Fig. 3(b): "broadcast and select and partial WDM multicast." In this structure a shared WDMult module is presented in pink block diagram. Compared with the first one, the OBPF is replaced by a BV-WSS used to block the undesired signals and select one single- or multi-channel signals which need WDM multicast. All of the input signals from each port are split to the shared WDMult module and the selected signals can achieve WDM multicast. This structure supports unicast, broadcast, and partial WDM multicast for single- or multi-channel signals at a low cost.

With the expansion of degrees in OXC, the aforementioned structures in Figs. 1(a) and 3(a) and (b) will result in increased power loss due to the use of couplers. To mitigate this problem, the structure in Fig. 1(b) is considered, and the input-side couplers are replaced with BV-WSSs. However, this structure only supports the functions of routing and selecting, incapable of WDM multicast or broadcast. Therefore, we propose a power-saving OXC structure as shown in Fig. 3(c): "route and selectand WDM multicast". In this structure the coupler is replaced by a route WDMult module (blue block diagram) capable of not only routing but also WDM multicast. The incoming signals sent into a BV-WSS have two options: WDM multicast or be routed directly. The multicast signals are demultiplexed by the other BV-WSS and routed to the destination port. This architecture enables unicast and single- or multi-channel WDM multicast in a power efficient way.

Compare with the OXCs in [5] and [21], our proposed structures equipped with all-optical signal processing module can efficiently avoid the wavelength conflict and decrease the network block probability. With the help of BV-WSS, the flexible OXC structures are more suitable for the future elastic optical networks. The proposed three OXC structures have distinctive features and are suitable for different scenarios. In addition to the above mentioned functions, all of the three WDMult modules may work as wavelength converters if only one pump is activated. According to the different requirements, WDMult module can achieve different functions, such as wavelength conversion with one pump, single-channel multicast with two or three pumps, and multi-channel multicast with two pumps. Through FWM in SOA, the multifunctional all-optical wavelength conversion and WDM multicast can effectively reduce the cost and improve the network resource efficiency.

4. Experimental Setup and Results

The experimental setup is displayed in Fig. 4. The coherent optical transmitter (Tektronix OM5110) capable of generating QPSK signals is driven by an arbitrary waveform generator (AWG) to provide a repeated PRBS with the length of $2^{15} - 1$ at 25 Gbps. The light sources of pumps and signals are from five tunable external cavity lasers (ECL-EXFO-FLS2800) with linewidths of less than 100 kHz. In this proof-of-concept experiment, two CW lasers (ECL1, ECL2) are coupled into a single IQ modulator to generate the dual-channel QPSK signals which are separated to different fibers using a 3-dB coupler and two optical bandpass filters (BPF), respectively. In order to emulate two unrelated QPSK signals, the two filtered signals are passed through an optical delay line (ODL) and a variable optical attenuator (VOA), respectively. The input signals and pumps of SOA can be multiplexed together by a BV-WSS (Finisar DWP9F), which has 10 ports (9 switching ports and 1 common port), a maximum insertion loss of 6.5 dBm, and the variable channel bandwidth of 12.5 to 500 GHz resolution according to ITU-T G.694.1. The BV-WSS can be controlled by the programmable software to select the wanted wavelengths

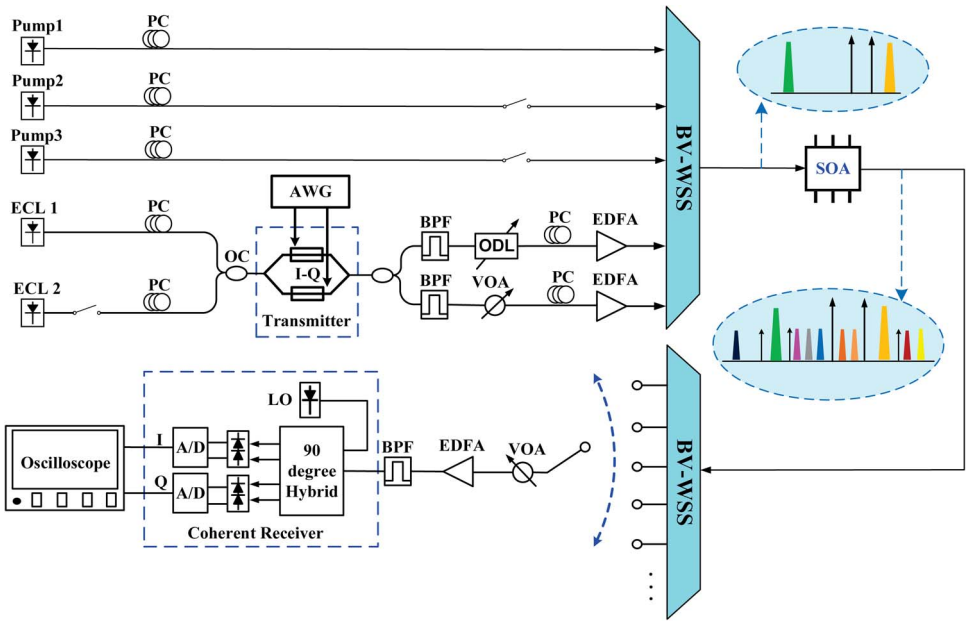

Fig. 4. Experiment setup: PC: polarization controller; OC: optical coupler; AWG: arbitrary waveform generator; BV-WSS: bandwidth variable wavelength selective switch; EDFA: erbium-doped fiber amplifier; VOA: variable optical attenuator; BPF: band-pass filter; ODL: optical delay line; A/D: analog to digital converter; LO: local oscillation.

and block the unwanted one. Therefore, according to different requirements, we can achieve wavelength conversion with one pump, WDM multicast with two or three pumps for single- or dual-channel signals. The coupled wavelengths are injected into the SOA (CIP-NL-OEC-1550) with a small signal gain of 34 dB and a saturation output power of 6 dBm. In order to achieve the best FWM efficiency, we should adjust the polarization state of the signals and pumps through the polarization controllers (PC). Then the desired wavelength conversion or WDM multicast are achieved via FWM in the SOA. The generated signals are demultiplexed by the other BV-WSS and every wavelength can be filtered to the corresponding output ports. The selected signal is detected by a coherent receiver (Tektronix OM4106D). The receiver sensitivity is measured before EDFA at the coherent receiver. Here, the EDFA as a pre-amplifier is set to the constant power mode to keep the input power of coherent receiver constant. Finally, constellation diagram, eye-diagram and bit-error rate (BER) measurements are obtained by a 33-GHz bandwidth oscilloscope (Tektronix MOS73304DX) and the optical spectra are observed by an optical spectra analyzer with the resolution of 0.05 nm (YOKOGAWA AQ6370B).

The single-channel wavelength conversion and one-to-six WDM multicast can be realized through FWM in SOA with one pump and two pumps, respectively. We have experimentally demonstrated these two schemes lately [18], [19], as shown in Fig. 5. This time, we further expand the research and mainly focus on WDM multicast with three pumps and dual-channel multicast schemes.

Firstly, we demonstrate the case of single-channel WDM multicast with three pumps $(P1, P2, P3)$ when the ECL2 is off. The wavelengths and powers of all inputs before the first BV-WSS are set as: $P1$ at 1544.1 nm with 3.0 dBm, $P2$ at 1548.1 nm with 3.5 dBm, $P3$ at 1554.9 nm with 3.5 dBm, and the input signal (S) at 1543.1 nm with 1.5 dBm. After the BV-WSS, one signal and three pumps are coupled together with the total power of 7.1 dBm and injected into the SOA with the bias current of 280 mA. The signal interacts with the pumps to simultaneously implement the D-FWM and ND-FWM. The spectrum at the output of SOA is shown in Fig. 6. After FWM, the phase information of input QPSK signal are delivered to the nine new generated idlers consisting of two degenerate components (f_{113}, f_{224}) and seven non-degenerate

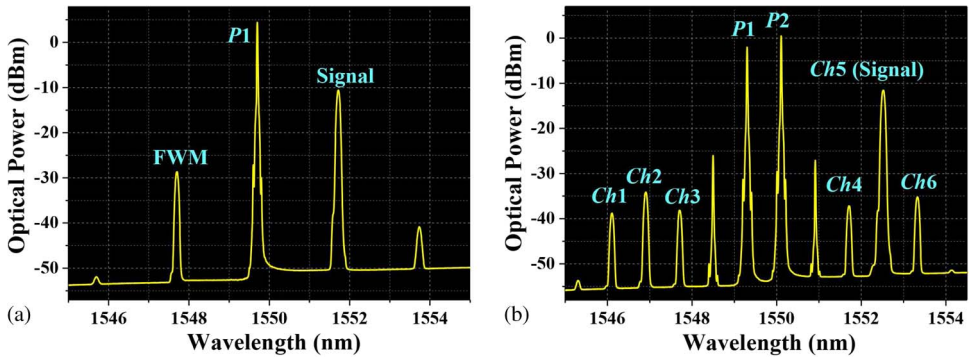

Fig. 5. Optical spectra of (a) wavelength conversion with one pump and (b) one-to-six WDM multicast with two pumps.

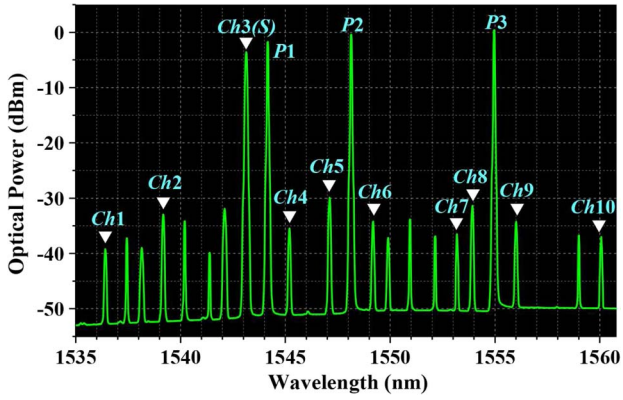

Fig. 6. Optical spectrum of one-to-ten WDM multicast with three pumps.

components $(f_{234}, f_{132}, f_{231}, f_{123}, f_{341}, f_{143}, f_{423})$, as analyzed above. In SOA, the FWM performs the complicated energy transfer process between the electric and optical energy, which results in the conversion efficiency (CE) may not be flat and optical signal-to-noise ratio (OSNR) may be spotty among ten channels $(Ch1, Ch2, \ldots, Ch10)$.

To characterize the performance of the three-pump multicast scheme, BER curves versus the received power for ten multicast channels are measured and shown in Fig. 7. All of the signals exhibit better BER performance than FEC threshold of 3.8×10^{-3}. The characteristics of ten multicast signals, including frequency label, wavelength, CE, OSNR, and power penalty at FEC threshold are summarized in Table 1. From the obvious comparison among the multicast signals, it is seen that the power penalty is inversely proportional to the OSNR, which is dependent on the CE and signal power. The frequency detuning, pump power, and bias current will affect the CE [15]. Due to the largest conversion range (0.7 nm), the CE and OSNR of $Ch10$ at f_{423} are relatively low compared with others and the largest power penalty of 1.7 dB is paid. The performance could be improved by optimizing the launched power and increasing the bias current. The concentrated constellations and clear eye-diagrams for both I and Q channels of the QPSK signals at the received power of -35 dBm is displayed in Fig. 8, which verifies the feasibility of the scheme.

Next, pmup3 is off and ECL2 is activated to implement the dual-channel WDM multicast with two pumps. The wavelength of ECL2 takes the place of the pmup3 and others are kept. ECL1 and ECL2 are coupled into a single IQ modulator to generate the dual-channel QPSK signals (S_A and S_B). The powers of two signals are both 1.0 dBm and the powers of two pumps are 4.5 dBm before the BV-WSS. After the BV-WSS, the total power of four coupled components

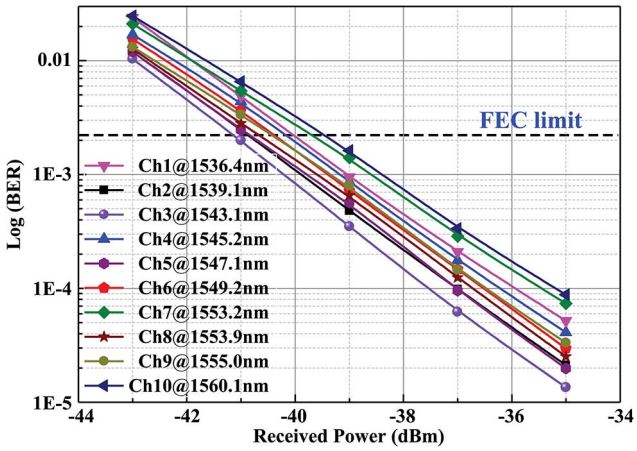

Fig. 7. Measured BER performance for the ten multicast signals.

TABLE 1

Summary of wavelength, frequency, conversion efficiency, OSNR, and power penalty

Channel Label	Frequency Label	Wavelength (nm)	CE (dB)	OSNR (dB)	Power penalty (dB)
$Ch1$	f_{234}	1536.4	-35.3	14.2	1.1
$Ch2$	f_{132}	1539.1	-29.4	19.4	0.3
$Ch3$	f_3	1543.1	\	47.5	0.0
$Ch4$	f_{113}	1545.2	-31.9	15.8	0.95
$Ch5$	f_{231}	1547.1	-26.3	21.2	0.28
$Ch6$	f_{123}	1549.2	-30.4	16.3	0.8
$Ch7$	f_{223}	1553.2	-33.5	13.5	1.45
$Ch8$	f_{341}	1553.9	-27.7	19.2	0.42
$Ch9$	f_{143}	1555.0	-30.5	16.0	0.9
$Ch10$	f_{423}	1560.1	-33.8	13.1	1.7

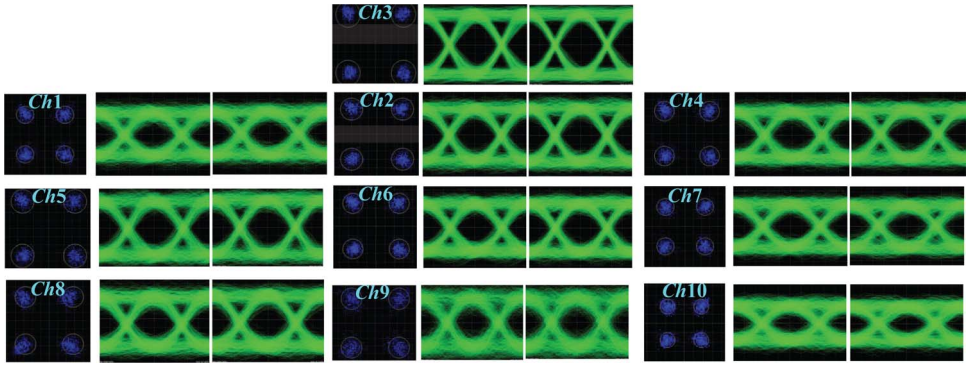

Fig. 8. The constellations and eye-diagrams of the ten multicast signals (measured at -35 dBm).

is 5.3 dBm. Through the FWM in SOA with the bias current of 300 mA, the replicated QSPK signal from S_A is obtained at f_{132}, f_{113}, f_{231}, f_{123}, and f_{223} (from A_1 to A_5); meanwhile, the one from S_B is copied to f_{124}, f_{142} (B_1, B_2), as shown in Fig. 9.

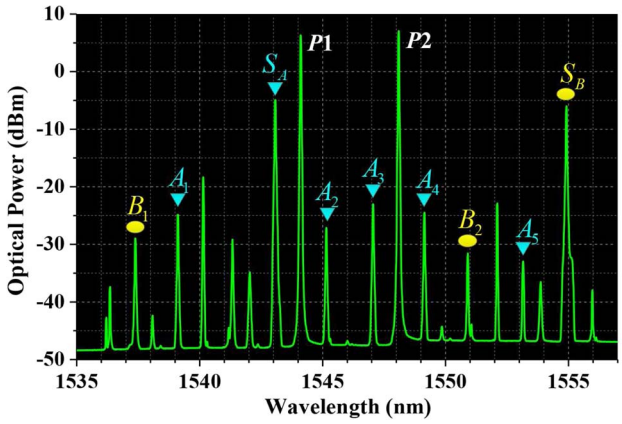

Fig. 9. Optical spectrum of dual-channel (one-to-six and one-to-three) WDM multicast with two pumps.

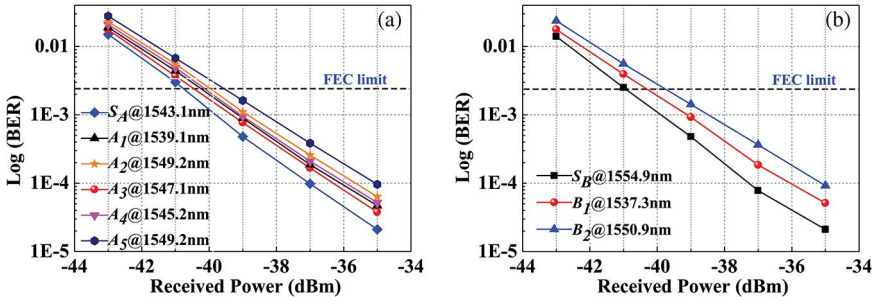

Fig. 10. Measured BER performance. (a) Six signals from S_A and (b) three signals from S_B.

Note that for dual-channel multicast scheme, the FWM process is more complicated. Two signals interact with each other and with two pumps. Therefore, many idlers will be generated including degenerate and non-degenerate components, which may cause the crosstalk. In order to avoid frequency overlap for the new generated idlers, the frequency detuning among four inputs need to be adjusted properly. Due to the larger frequency interval between S_B and two pumps, the other generated idlers from S_B have the relatively low conversion efficiencies compared with B_1 and B_2. Therefore, we only select two idlers for S_B as the multicast signals and abandon others with the modest performance. Finally, including the original signals, the one-to-six and one-to-three multicast for dual-channel signals are simultaneously achieved. In the practical application, the fold numbers of multicast for different services are always different [23]. Therefore, even though the fold numbers for two input signals are not equal, the proposed scheme can still meet most of multicast requirements.

Fig. 10 presents the BER curves of the multicast signals as a function of the received power. The original signals S_A and S_B are also measured as references. All of the generated components exhibit better performance than FEC threshold. The characteristics of the multicast signals including frequency label, wavelength, CE, OSNR, and power penalty at FEC limit are summarized in Table 2. Due to the largest conversion range (10.1 nm), the A_5 at f_{223} has the lowest CE and OSNR with the power penalty of 1.28 dB. The polarization angle between P_1 and S_B, P_2 and S_B results in the relatively lower CE and OSNR with the power penalty of 1.27 dB. The polarization sensitivity is mainly due to the fact that FWM efficiency is dependent on the relative polarization state between the injected beams [24]. We also measure the corresponding constellations and I/Q eye-diagrams of the two original signals and seven converted signals, as shown in Fig. 11. The concentrated constellation and clear open eye-diagrams prove the good quality of QPSK signals.

TABLE 2

Summary of wavelength, frequency, conversion efficiency, OSNR, and power penalty

Channel Label	Frequency Label	Wavelength (nm)	CE (dB)	OSNR (dB)	Power penalty (dB)
S_A	f_3	1543.1	\	43.1	0.0
A_1	f_{132}	1539.1	−17.9	23.3	0.54
A_2	f_{113}	1545.2	−22.1	20.6	0.82
A_3	f_{231}	1547.1	−17.7	24.5	0.31
A_4	f_{123}	1549.2	−19.3	22.7	0.67
A_5	f_{223}	1553.2	−27.8	14.2	1.28
S_B	f_4	1554.9	\	41.2	0.0
B_1	f_{124}	1537.3	−22.8	19.2	0.78
B_2	f_{142}	1550.9	−25.4	14.3	1.27

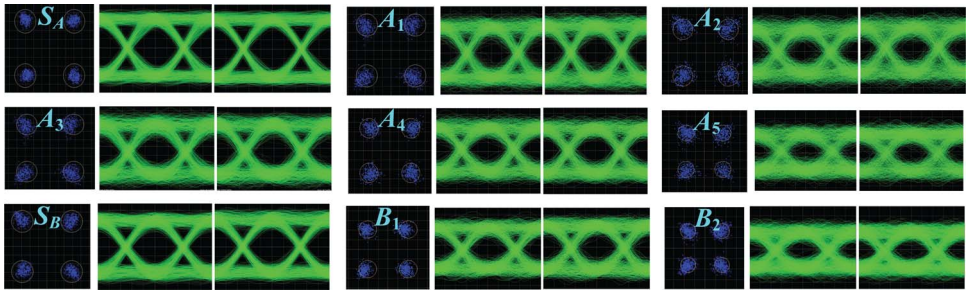

Fig. 11. The constellations and eye-diagrams of dual-channel WDM multicast signals (measured at −35 dBm).

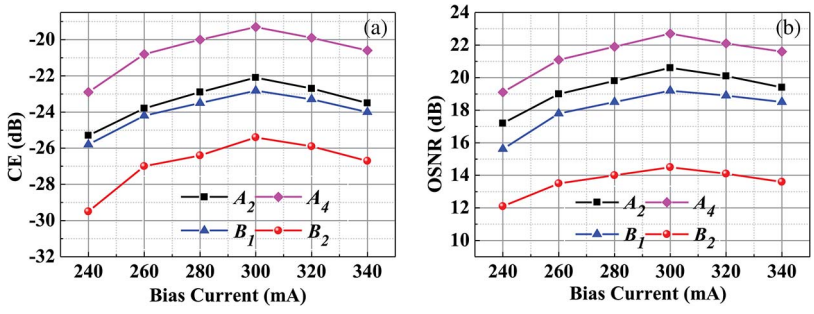

Fig. 12. (a) CE and (b) OSNR of four selected multicast signals (A_2, A_4, B_1, B_2) under different bias currents.

In addition, the bias current of SOA also has the large effect on the performance of signals. Therefore, we investigate the influence of bias current on CE and OSNR. The bias current is adjusted from 240 to 340 mA and other conditions are kept. We select four idlers (A_2, A_4, B_1, B_2) to analyze the effect of the bias current on CE and OSNR, as shown in Fig. 12. When the bias current is small, the CE and OSNR are improved as the bias current rises. That is because larger bias current provides higher carrier density which leads to higher CE and OSNR. However, when the bias current reaches a certain value, the CE and OSNR start to deteriorate as bias current rises. It is mainly because too large bias current generates high-order FWM components. The

high-order FWM idlers consume the energy from pumps and current, which leads to a decline in CE and OSNR of multicast signals. Moreover, the high-order FWM may cause the crosstalk to the other multicast signals which will further damage the signal performance. The optimum bias currents for multicast signals from S_A and S_B are both 300 mA.

Through the experiment, we have demonstrated the feasibility of wavelength conversion, one-to-six, one-to-ten, and dual-channel WDM multicast. The proposed three OXCs are designed for our demonstrated physical experiments based on FWM in SOA. Therefore, they can be applied into the corresponding OXC structure according to the different requirements. Meanwhile, the experimental setup can be flexibly converted into the corresponding WDMult modules in OXCs by simply modifying some parts of the setup. We think that implementing the all-optical signal processing technology in the practical scenario will be a target of the future all-optical communications.

5. Conclusion

We have proposed three OXC structures equipped with the WDM multicast module. The three OXC structures had distinctive features and were suitable for different scenarios. Based on FWM, one-to-ten WDM multicast of 25 QPSK signals were demonstrated by applying three pumps in SOA. Moreover, one-to-six and one-to-three dual-channel WMD multicast for the two original signals were simultaneously achieved. Less than 1.7 dB power penalty for all of the multicast signals was successfully observed. The influence of bias current on CE and OSNR was also discussed and the optimal value was given. With the development of WDM multicast technology, more various devices, more folds, higher order modulation formats, faster bit rates, more channels, and more flexible control will be realized. Therefore, we believe that the OXC structures with the ability of WDM multicast will be more and more critical and indispensable in the future.

References

[1] P. Kirci and A. H. Zaim, "WDM network and multicasting protocol strategies," *Sci. World J.*, vol. 2014, 2014, Art. ID. 581052.
[2] P. Jia, Y. Liang, S. Huang, J. Zhang, and W. Gu, "Multicast with a new switching structure in optical networks," *Photon. Netw. Commun.*, vol. 15, no. 1, pp. 83–89, Feb. 2008.
[3] X. Yu, G. Xiao, and T. H. Cheng, "An efficient mechanism for dynamic multicast traffic grooming in overlay IP/MPLS over WDM networks," *Opt. Fiber Technol.*, vol. 20, no. 4, Aug. 2014.
[4] L. H. Sahasrabuddhe and B. Mukherjee, "Light trees: Optical multicasting for improved performance in wavelength routed networks," *IEEE Commun. Mag.*, vol. 37, no. 2, pp. 67–73, Feb. 1999.
[5] M. Ali and J. S. Deogun, "Power-efficient design of multicast wavelength-routed networks," *IEEE J. Sel. Areas Commun.*, vol. 18, no. 10, pp. 1852–1862, Oct. 2000.
[6] D. D. Le, M. Molnár, and J. Palaysi, "Multicast routing in WDM networks without splitters," *IEEE Commun. Mag.*, vol. 52, no. 7, pp. 158–167, Jul. 2014.
[7] K. Chow and C. Shu, "All-optical signal regeneration with wavelength multicasting at 6 × 10 Gb/s using a single electroabsorption modulator," *Opt. Exp.*, vol. 12, no. 13, pp. 3050–3054, Jun. 2004.
[8] Z.-Q. Hui, "All-optical 1-to-8 wavelength multicasting at 20 Gbit/s exploiting self-phase modulation in dispersion flattened highly nonlinear photonic crystal fiber," *Sci. World J.*, vol. 2014, 2014, Art. ID. 828179.
[9] G. Contestabile *et al.*, "All-optical wavelength multicasting in a QD-SOA," *IEEE J. Quant. Electron.*, vol. 47, no. 4, pp. 541–547, Apr. 2011.
[10] M. Pu *et al.*, "One-to-six WDM multicasting of DPSK signals based on dual-pump four-wave mixing in a silicon waveguide," *Opt. Exp.*, vol. 19, no. 24, pp. 24 448–24 453, Nov. 2011.
[11] M. P. Fok and C. Shu, "Performance investigation of one-to-six wavelength multicasting of ASK–DPSK signal in a highly nonlinear bismuth oxide fiber," *J. Lightw. Technol.*, vol. 27, no. 15, pp. 2953–2957, Aug. 2009.
[12] Z. Chen *et al.*, "One-to-nine multicasting of RZ-DPSK based on cascaded four-wave mixing in a highly nonlinear fiber without stimulated Brillouin scattering suppression," *IEEE Photon. Technol. Lett.*, vol. 24, no. 20, pp. 1882–1885, Oct. 2012.
[13] M. Fok and C. Shu, "Multipump four-wave mixing in a photonic crystal fiber for 6 × 10 Gb/s wavelength multicasting of DPSK signals," *IEEE Photon. Technol. Lett.*, vol. 19, no. 15, pp. 1166–1168, Aug. 2007.
[14] Y. Xie, S. Gao, and S. He, "All-optical wavelength conversion and multicasting for polarization-multiplexed signal using angled pumps in a silicon waveguide," *Opt. Lett.*, vol. 37, no. 11, pp. 1898–1900, Jun. 2012.
[15] D. Wang *et al.*, "Performance comparison of using SOA and HNLF as FWM medium in a wavelength multicasting scheme with reduced polarization sensitivity," *J. Lightw. Technol.*, vol. 28, no. 24, pp. 3497–3505, Dec. 2010.

[16] B. Filion, S. Amiralizadeh, A. T. Nguyen, L. A. Rusch, and S. LaRochelle, "Wideband wavelength conversion of 16 Gbaud 16-QAM signals in a semiconductor optical amplifier," presented at the Opt. Fiber Commun. Conf., Anaheim, CA, USA, Mar. 17–21, 2013, Paper OTh1C-5.
[17] B. Filion, W. Ng, A. T. Nguyen, L. A. Rusch, and S. LaRochelle, "Wideband wavelength conversion of 16 Gbaud 16-QAM and 5 Gbaud 64-QAM signals in a semiconductor optical amplifier," *Opt. Exp.*, vol. 21, no. 17, pp. 19 825–19 833, Aug. 2013.
[18] D. Wang *et al.*, "Optical network node supporting one-to-six WDM multicasting of QPSK signals," *IEEE Photon. Technol. Lett.*, vol. 26, no. 16, pp. 1641–1644, Aug. 2014.
[19] D. Wang *et al.*, "Multifunctional switching unit for add/drop, wavelength conversion, format conversion, and WDM multicast based on bidirectional LCoS and SOA-loop architecture," *Opt. Exp.*, vol. 22, no. 18, pp. 21 847–21 858, Sep. 2014.
[20] A. Malacarne *et al.*, "Optical multicasting of 16QAM signals in periodically-poled lithium niobate waveguide," *J. Lightw. Technol.*, vol. 31, no. 11, pp. 1797–1803, Jun. 2013.
[21] Y. Tanaka, H. Hasegawa, and K.-I. Sato, "Performance evaluations of large-scale OXC that achieves modular and hitless expansion," presented at the Opt. Fiber Commun. Conf., San Francisco, CA, USA, Mar. 9–13, 2014, Paper No. W2A-50.
[22] A. E. Willner, S. Khaleghi, M. R. Chitgarha, and O. F. Yilmaz, "All-optical signal processing," *J. Lightw. Technol.*, vol. 32, no. 4, pp. 660–680, Feb. 2014.
[23] T. Rahman, G. Ellinas, and M. Ali, "Lightpath- and light-tree-based groupcast routing and wavelength assignment in mesh optical networks," *J. Opt. Commun. Netw.*, vol. 1, no. 2, pp. A44–A55, Jul. 2009.
[24] J. P. Lacey, M. A. Summerfield, and S. Madden, "Tunability of polarization-insensitive wavelength converters based on four-wave mixing in semiconductor optical amplifiers," *J. Lightw. Technol.*, vol. 16, no. 12, pp. 2419–2427, Dec. 1998.